Alterations of the Gut Microbiota in Patients with COVID-19 or H1N1 Influenza

Silan Gu[1*], Yanfei Chen[1*], Zhengjie Wu[1*], Yunbo Chen[1*], Hainv Gao[2], Longxian Lv[1],

Feifei Guo[2], Xuewu Zhang[3], Rui Luo[1], Chenjie Huang[1], Haifeng Lu[1], Beiwen Zheng[1],

Jiaying Zhang[1], Ren Yan[1], Hua Zhang[1], Huiyong Jiang[1], Qiaomai Xu[1], Jing Guo[1],

Yiwen Gong[1], Lingling Tang[2#] and Lanjuan Li[1]

Author affiliations

1. State Key Laboratory for Diagnosis and Treatment of Infectious Diseases, National Clinical Research Center for Infectious Diseases, Collaborative Innovation Center for Diagnosis and Treatment of Infectious Diseases, The First Affiliated Hospital, College of Medicine, Zhejiang University, Hangzhou, 310003, China

2. Department of Infectious Diseases, Shulan (Hangzhou) Hospital, Affiliated to Shulan International Medical College, Zhejiang Shuren University, Hangzhou 310003, China

3. Department of Hematology, The First Affiliated Hospital, College of Medicine, Zhejiang University, Hangzhou 310003, China

SG, YC, ZW and YC joint first coauthorship.

LT and LL joint last coauthorship.

Contact information

Corresponding author:

Lanjuan Li (ljli@zju.edu.cn)

State Key Laboratory for Diagnosis and Treatment of Infectious Diseases, National

Clinical Research Center for Infectious Diseases, Collaborative Innovation Center for Diagnosis and Treatment of Infectious Diseases, The First Affiliated Hospital, College of Medicine, Zhejiang University, Hangzhou, 310003, China.

Summary

In this cross-sectional study, we identified specific signatures of the fecal microbiota in COVID-19 patients, H1N1 patients, and healthy controls in a Chinese population by high-throughput 16S rRNA gene sequencing to provide a theoretical basis for intestinal microbial intervention.

Abstract

Background. Coronavirus disease 2019 (COVID-19) is an emerging serious global health problem. Gastrointestinal symptoms are common in COVID-19 patients, and SARS-CoV-2 RNA has been detected in stool specimens. However, the relationship between the gut microbiome and disease remains to be established.

Methods. We conducted a cross-sectional study of 30 COVID-19 patients, 24 influenza A (H1N1) patients, and 30 matched healthy controls (HC) to identify differences in the gut microbiota by 16S ribosomal RNA (rRNA) gene V3-V4 region sequencing.

Results. Compared with HC, COVID-19 patients had significantly reduced bacterial diversity, a significantly higher relative abundance of opportunistic pathogens, such as *Streptococcus, Rothia*, *Veillonella* and *Actinomyces,* and a lower relative abundance of beneficial symbionts. Five biomarkers showed high accuracy for distinguishing COVID-19 patients from HC with an area under the curve (AUC) up to 0.89. Patients with H1N1 displayed lower diversity and different overall microbial composition compared with COVID-19 patients. Seven biomarkers were selected to distinguish the two cohorts with an AUC of 0.94.

Conclusion. The gut microbial signature of patients with COVID-19 was different from that of H1N1 patients and HC. Our study suggests the potential value of the gut microbiota as a diagnostic biomarker and therapeutic target for COVID-19, but further validation is needed.

Keywords. COVID-19, H1N1, intestinal microbiota, dysbiosis, biomarker.

INTRODUCTION

Coronavirus disease 2019 (COVID-19) is an emerging respiratory infectious disease caused by severe acute respiratory syndrome coronavirus 2 (SARS-CoV-2), and rapidly spread throughout the world[1]. The clinical manifestations and transmission routes of seasonal influenza A (H1N1) are similar to those of COVID-19[2, 3]. WHO reported that the prevalence of influenza and influenza-like illness were high in China and the United States in the 2019-2020 season[4]. Distinguishing COVID-19 and H1N1 at the early stage of outbreaks is essential because occupational safety measures, treatment, and prognosis are different between these entities.

SARS-CoV-2 binds to angiotensin-converting enzyme 2 (ACE2) receptors to invade human cells, and these receptors are highly expressed in the intestinal epithelium[5]. ACE2 might be associated with cardiopulmonary disease via alterations in the gut and/or lung microbiomes[6]. Previous studies have found that 3.34-11.4% of COVID-19 patients had gastrointestinal symptoms, such as vomiting and diarrhea, especially in critically ill patients[7, 8]. Moreover, viral RNA and live viruses were detected in fecal samples, suggesting that the digestive tract might be a site of viral replication and activity[9]. However, the interaction between COVID-19 and intestinal microorganisms is not fully understood.

The intestinal flora is involved in host nutrient absorption and metabolism and has a profound impact on human health and disease[10-12]. Previous studies indicated that the intestinal flora was closely related to respiratory virus infection and could affect the occurrence and development of diseases through the gut-lung axis[13]. Moreover, influenza infection can affect the composition of the intestinal microbiota[14], and intestinal microflora disorders reduce host antiviral immune response, thereby aggravating lung damage caused by these infections[15].

This cross-sectional study analyzed the gut microbiome of COVID-19 patients, H1N1 patients, and healthy controls (HC) by high-throughput sequencing of the 16S rRNA gene to provide a theoretical basis for differential diagnosis and intestinal microbial intervention. The results showed that biomarkers could be used to identify changes in the structure, composition, and function of the microbiome between these

patient groups.

MATERIALS and METHODS

Study Design and Enrolled Patients

The study was approved by the Research Ethics Committee of the First Affiliated Hospital of the Zhejiang University School of Medicine (No. IIT2020-136 and 2018-447). A cohort of 84 subjects was recruited, including 30 COVID-19 patients, 24 hospitalized patients with H1N1 infection, and 30 age-, gender-, and BMI-matched HC who met the inclusion criteria described in our previous study[16].

The COVID-19 patients were admitted to the First Affiliated Hospital of the Zhejiang University School of Medicine between January 2020 and March 2020. Disease severity was classified into four types according to the diagnostic criteria of the seventh edition of the Diagnostic and Treatment Protocol for COVID-19 in China[17], and our cohort presented either (1) general disease, characterized by fever, respiratory symptoms, and lung imaging evidence of pneumonia; or (2) severe disease, manifested by a respiratory rate (RR) ≥30 per min, oxygen saturation ≤ 93% at rest, arterial partial pressure of oxygen (PaO_2)/fraction of inspired oxygen (FiO_2) ≤300 mmHg, or progression (>50%) in lung imaging lesions within 24–48 h.

H1N1 patients hospitalized from January 2018 to March 2019 were enrolled. According to the WHO surveillance case definitions for severe acute respiratory infection (SARI), the degree of severity of H1N1 in our cohort was classified as severe at the time of admission[18].

All subjects who received antibiotics, probiotics, or both within 4 weeks before enrollment were excluded. Viral infections were confirmed by real-time reverse-transcription polymerase chain reaction. Only laboratory-confirmed cases with clinical symptoms were included in the study.

Patient data, including laboratory test results, clinical manifestations, and disease course, were obtained from medical records and laboratory information systems.

Sample Collection and Processing

Fecal samples from COVID-19 and H1N1 patients were collected at admission,

and fresh stools from healthy subjects were collected during physical examination. Fecal samples were processed in the laboratory within 4 hours after collection and stored at -80°C until analysis.

Blood samples were taken from all study subjects for analyzing hematological variables, liver functions, kidney functions and serum cytokines, using routine clinical laboratory methods as described in the Supplementary Methods.

DNA Extraction

Given the potential presence of live virus in feces, all fecal samples were inactivated at 56°C for 30 min before DNA extraction. Microbial DNA was extracted from 200 mg feces per sample using DNeasy PowerSoil Pro Kit (Qiagen, California, USA) with a bead-beating step according to the manufacturer's protocol, as described elsewhere[19].

Sequencing and Bioinformatics

DNA libraries were generated from PCR amplicons targeting the hypervariable regions V3-V4 of the 16S rRNA gene and sequencing using the Illumina MiSeq PE300 instrument (Illumina, San Diego, California, USA). Further details of sequencing protocol are available in Supplementary Methods.

The raw sequencing reads were quality-filtered and merged by Trimmomatic and FLASH. Operational taxonomic units (OTUs) with a similarity cut-off of 97% were clustered using UPARSE version 7.1 (http://drive5.com/uparse), and chimeric sequences were identified and removed. After filtering, an average of 48,879 reads per sample was obtained (minimum, 33,476; maximum, 63,480). The taxonomy of each OTU representative sequence was analyzed by RDP Classifier (http://rdp.cme.msu.edu/) against the 16S rRNA database (Silva SSU132). Alpha diversity was assessed using the Chao 1 index and Shannon index. Beta diversity was estimated by the Bray-Curtis distance and was visualized by principal coordinate analysis (PCoA).

For biomarker identification, a two-step approach was adopted. First, a random forest model[20] was constructed for distinguishing between the two groups, and ten most predominant genera as candidate biomarkers were selected on the basis of

importance values (using the R package "randomForest", ntree=500) (Supplementary Table S1). Second, the differences in taxonomic composition taxa between two cohort groups were identified using the linear discriminant analysis (LDA) effect size (LEfSe) analysis (http://huttenhower.sph.harvard.edu/galaxy/). Candidate biomarkers with a LDA>3.5 were selected as final biomarkers. The discriminatory ability of the biomarkers was evaluated by plotting receiver-operating characteristic (ROC) curves and calculating the area under the ROC curve (AUC) using R software's pROC package.

Statistical Analysis

Continuous variables were reported as means ± standard deviations, and statistical comparisons were made using the independent t-test. Non-normally distributed variables were expressed as interquartile range (IQR), and comparisons were conducted using the Mann-Whitney U test. For correlation analysis, Spearman's rank test was performed. Statistical analysis was performed using SPSS version 20.0 (SPSS Inc., Chicago, IL). *P* values of less than 0.05 after multiple-comparison correction using the false discovery rate method were considered significant.

RESULTS

Clinical Characteristics of the Study Population

The study population included 30 hospitalized patients with confirmed SARS-CoV-2 infection, 24 hospitalized patients with confirmed H1N1 infection, and 30 healthy subjects. Clinical data are shown in Table 1. The median age of COVID-19 patients was 55 years (IQR, 48-62; range, 29-70 years), and 13 (43.3%) were women. The median duration of hospitalization was 16.0 days (IQR, 12.0–21.3). In this group, 33.3% had at least one coexisting medical condition, and the most common comorbidity was hypertension (30.0%). Fever was present in 86.7% of the patients on admission, and the median body temperature was 38.2 ℃ (IQR, 37.5–38.8). Five patients (16.7%) presented with diarrhea.

There were no significance differences in age, gender, and body mass index (BMI) between the groups. However, there were significant differences in platelet

count, aspartate aminotransferase (AST), IL-4, and TNF-α between H1N1 and COVID-19 patients ($P<0.05$). The rate of hypertension did not differ significantly between these two groups ($P=0.445$). With regard to inflammatory markers, there was a significant difference in procalcitonin ($P=0.016$) but no significant difference in C-reactive protein (CRP) ($P=0.832$) between H1N1 and COVID-19 patients. There were significant differences in lymphocyte count, alanine aminotransferase (ALT), IL-2, IL-4, IL-6, IL-10 and TNF-α between HC and COVID-19 patients.

According to clinical guidelines, COVID-19 severity on admission was categorized as general in 15 patients and severe in 15 patients. The clinical data of these subjects were summarized and compared (Supplementary Table S2). There was a significant difference in white blood cell (WBC) count, neutrophil count, lymphocyte count, and lactate dehydrogenase (LDH) between these two groups ($P<0.05$).

Microbial Diversity is Decreased in COVID-19 and H1N1 Patients

The characteristics of the gut microbiome in patients with respiratory virus infections were analyzed by 16S rDNA gene sequencing of 84 fecal samples (one sample per patient). After merging and filtering, 4,105,869 high-quality sequence reads were generated, with an average of 48,879 sequences per sample for subsequent data analysis.

The mean community richness and microbial diversity were significantly lower in COVID-19 and H1N1 patients than in HC, according to Shannon diversity index and Chao diversity index (Figures 1A, B). The number of OTUs in the COVID-19, H1N1, and HC groups was 911, 960, and 922, respectively. More than 50% of 1242 OTUs were shared by the three groups, and 62.3% of OTUs overlapped between the COVID-19 group and HC (Figure 1C). PCoA of Bray-Curtis distances indicated differences in the fecal microbiota between COVID-19 and H1N1 patients and between these groups and HC (ANOSIM, R=0.36, p=0.001) (Figure 1D). Ternary plot showed that the relative abundance of *Streptococcus* and *Escherichia-Shigella* was significantly higher in COVID-19 and H1N1 patients, respectively (Figure 1E).

The analysis of group similarities indicated that differences in richness, diversity,

and structure of the gut microbiota were not significantly different between general and severe COVID-19 patients (ANOSIM, p=0.426; Supplementary Figure S1), indicating that the experimental design was adequate.

Bacterial Taxonomic Differences Among the Three Groups

To investigate changes in the microbiota of COVID-19 patients, we assessed relative abundance in the three groups at the phylum, class, family, and genus levels (Figure 2). At the phylum level, the relative abundance of phyla *Actinobacteria* and *Firmicutes* significantly decreased in the H1N1 group compared with the COVID-19 group and HC, which was largely due to a significant reduction in class Actinobacteria, Erysipelotrichia, and Clostridia. At the family level, the amount of several representative groups of putative anaerobic butyrate-producing bacteria (BPB) from the families *Lachnospiraceae* and *Ruminococcaceae* was dramatically decreased in H1N1 patients. This result was partly due to significant depletion in the abundance of *Blautia*, *Agathobacter*, *Anaerostipes*, *Fusicatenibacter*, *Eubacterium hallii group*, unclassified *Lachnospiraceae*, *Dorea*, *Faecalibacterium*, and *Ruminococcus-2* in the H1N1 group. Similarly, compared with HC, the abundance of the *Ruminococcaceae* family and several genera from the *Lachnospiraceae* family (*Fusicatenibacter*, *Anaerostipes*, *Agathobacter*, unclassified *Lachnospiraceae*, and *Eubacterium hallii group*) was dramatically reduced in COVID-19 patients. However, the number of *Streptococcus* (class Bacilli) was higher in COVID-19 patients than in the other two groups.

Differences in the Fecal Microbiota across All Groups

LEfSe analysis was used to determine and distinguish the composition of the gut microbiome between the COVID-19 group and HC. The gut microbiome of the COVID-19 group was dominated by *Streptococcus*, *Rothia*, *Veillonella*, *Erysipelatoclostridium*, and *Actinomyces*, whereas the microbiome of HC was dominated by the genera *Romboutsia*, *Faecalibacterium*, *Fusicatenibacter*, and *Eubacterium hallii group* (Figure 3A). Spearman correlation analysis was performed to evaluate relationships among genera (Figure 3B). There were significant positive correlations across COVID-19-enriched genera. However, there was a negative

correlation between genera enriched in the COVID-19 group and HC. Five final biomarkers (*Fusicatenibacter, Romboutsia, Intestinibacter, Actinomyces, Erysipelatoclostridium*) were selected to distinguish between the COVID-19 group and HC, with ROC-plot AUC value of 0.89 (95% CI, 0.8–0.97) (Figure 3C).

The effect of viral infections on the intestinal flora was determined by comparing estimated fecal microbiome phylotypes in H1N1 patients and HC by LEfSe analysis (Supplementary Figure S2). The microbiome of the H1N1 group was dominated by *Enterococcus*, *Prevotella*, *Finegoldia* and *Peptoniphilus*, whereas the microbiome of HC had a dominance of *Blautia*, *Romboutsia*, *Collinsella*, *Bifidobacterium*, and other beneficial bacteria. Six final biomarkers (*Fusicatenibacter*, *Romboutsia*, *Anaerostipes*, *Eubacterium hallii group*, *Ruminococcus torques group*, and *Blautia*) were selected to differentiate the H1N1 group and HC, and the AUC was 0.95 (95% CI, 0.89–1.00) (Supplementary Figure S2).

Differences in the Fecal Microbiota between COVID-19 and H1N1 Patients

The gut microbiota signature of COVID-19 and H1N1 patients was analyzed to assess correlations between disease characteristics and the microbiome. The abundance of *Prevotella*, *Ezakiella*, *Murdochiella*, and *Porphyromonas* was higher in the H1N1 group than in COVID-19 patients (Figure 4A). In addition, seven final biomarkers (*Streptococcus*, *Fusicatenibacter*, *Collinsella*, *Dorea*, *Agathobacter*, *Eubacterium hallii group*, *Ruminococcus torques group*) were selected reference the two-step schema in the method to distinguish the two cohorts, with an AUC of 0.94 (95% CI, 0.87–1.00) (Figure 4B).

Relationship between Gut Microbiota Composition and Clinical Indexes

Spearman analysis was conducted to evaluate the correlation between genera (abundance >0.1%) and clinical indexes, including WBC, CRP, PCT, D-dimer, IL-2, IL-4, IL-6, and TNF-α in COVID-19 and H1N1 patients, respectively. The significance thresholds were absolute correlation coefficients higher than 0.4 and *P* values lower than 0.05, as shown in Figure 5.

Compared with HC, *Agathobacter*, *Fusicatenibacter*, *Roseburia* and *RuminococcaceaeUCG−013* were depleted in COVID-19 patients and were

negatively correlated mainly with CRP, PCT or D-dimer levels. Moreover, CRP and D-dimer levels were positively correlated with COVID-19-enriched bacteria (*Streptococcus*, *Rothia*, *Veillonella*, and *Actinomyces*) (Figure 5A). In addition, there was a positive correlation between inflammatory cytokines IL-2, IL-4, IL-6 and the abundance of H1N1-enriched bacteria (*Finegoldia*, *Anaerococcus*, *Peptoniphilus*, *Intestinibacter*, and *Prevotella*) (Figure 5B).

DISCUSSION

COVID-19 is a serious global health problem. As of 22 May 2020, more than 5 million confirmed infections were reported worldwide, with over 330,000 deaths[21]. The epidemic has increased awareness of the importance of life, health, and public health. However, differentiating COVID-19 from other respiratory infectious diseases is challenging, especially during influenza season[22, 23]. In this cross-sectional study, we identified specific signatures of the fecal microbiota in COVID-19 patients, H1N1 patients, and HC in a Chinese population.

Compared with HC, COVID-19 patients had a significantly lower lymphocyte count and a significantly higher level of IL-6 and TNF-α, which agrees with previous findings[2]. Our results showed that clinical manifestations were similar between H1N1 and COVID-19 patients, and a wider range of detection might be necessary when etiology is identified.

There was a significant decrease in gut microbiota diversity and abundance in COVID-19 and H1N1 patients compared with HC, which is consistent with previous studies[24, 25], in which low bacterial diversity was associated with respiratory viral infectious diseases. Moreover, there were significant disease-specific shifts in the overall microbiota composition between COVID-19 and H1N1 patients and HC.

One of the most striking findings was the increased relative abundance of opportunistic pathogens, including *Streptococcus*, *Rothia*, *Veillonella*, *Erysipelatoclostridium*, and *Actinomyces* in COVID-19 patients, and these taxa were positively associated with CRP, the index of bacterial infection. Mortality from SARI is higher in middle-aged and older adults with underlying diseases, and secondary

bacterial infections are an important cause of death[2]. *Rothia* is thought to contribute to the pathogenesis of pneumonia, especially in immunocompromised individuals and patients with retained catheters[26]. Our previous study suggested that *Streptococcus* and *Rothia* were associated with susceptibility to secondary bacterial lung infection in patients with avian H7N9 virus infection[27]. Other studies have revealed that changes in the enteric environment and immune factors caused by *Actinomyces* may aggravate the damage caused by inflammatory bowel disease[28, 29]. In addition, the abundance of BPB decreased whereas the opportunistic pathogens *Prevotella*, *Finegoldia*, and *Peptoniphilus* were enriched in H1N1 patients in our cohort, as observed in H7N9 patients[30]. Noteworthily, the levels of IL-2 and IL-4 significantly increased in H1N1 patients and highly positively correlated with these enriched bacteria, while their causal relationship needs further explore.

Increasing evidence indicates the intimate relationship between the gastrointestinal and respiratory tract, which is known as the gut-lung axis[13]. Deriu found that influenza infection alters the intestinal microbial profile through a mechanism dependent on type I interferons (IFN-Is) induced in the pulmonary tract[31]. Respiratory influenza infection caused intestinal injury when lung injury occurred, by recruiting lung-derived $CCR9^+CD4^+$ T cells to the small intestine and stimulating the production of IFN-γ by these cells[14]. Studies have identified SARS-CoV-2 RNA in stool specimens of infected patients[9], and RNA analysis demonstrated that the duration of viral shedding from stool was longer than that from respiratory samples[32]. In addition, host ACE2 receptors are highly expressed in the gastrointestinal epithelium[7]. SARS-CoV-2 may interfere with nutrient absorption by binding to ACE2 receptors, causing gastroenteritis-like symptoms, and disrupting intestinal homeostasis.

Another important finding was the significant depletion of BPB in our cohort, especially in H1N1 patients versus HC. Previous studies have demonstrated the importance of BPB, which may be involved in the inflammatory mechanism of viral pneumonia[33, 34]. Studies showed that a high-fiber diet increased the production of short-chain fatty acids (SCFAs), enhanced antiviral $CD8^+$ T cell immune response

during influenza virus infection, and attenuated neutrophil-mediated lung injury, consequently improving survival[15, 35]. In turn, significantly reduced levels of BPB and other commensal bacteria with important physiological functions may promote the overgrowth of intestinal conditional pathogenic bacteria and increase both intestinal mucosal permeability and endotoxin concentrations in the blood, ultimately triggering inflammation, which exacerbates cytokine release[36, 37].

Several limitations of this study should be mentioned. Firstly, this was a single-center, cross-sectional study, with small sample size. Variations among patients at different disease stages of COVID-19 and H1N1 have not been evaluated. Secondly, although the participants were matched for age, sex ratio and BMI, gut microbiota can be influenced by other variables, such as diet and lifestyle parameters. Thirdly, while the changes observed in our study are obvious and reproducible, a mechanism that linked viral lung infection with changes in the gut microbiota was not identified.

In summary, we identified significant changes in gut microbial communities in COVID-19 and H1N1 patients and relevant biomarkers of these diseases. Moreover, there were significant changes in the structure and composition of the gut microbiome between these study groups. Specific microbial biomarkers of COVID-19 and H1N1 patients were identified and were correlated with clinical indexes. Notwithstanding, microbial signatures in COVID-19 and H1N1 patients need to be validated in larger cohorts, including subgroups at different stages of the disease.

Funding

Conflict of Interest

We declare no competing interests.

References

1. Chan JF, Yuan S, Kok KH, et al. A familial cluster of pneumonia associated with the 2019 novel coronavirus indicating person-to-person transmission: a study of a family cluster. Lancet **2020**; 395(10223): 514-23.

2. Huang C, Wang Y, Li X, et al. Clinical features of patients infected with 2019 novel coronavirus in Wuhan, China. Lancet **2020**; 395(10223): 497-506.

3. Iuliano AD, Roguski KM, Chang HH, et al. Estimates of global seasonal influenza-associated respiratory mortality: a modelling study. Lancet **2018**; 391(10127): 1285-300.

4. WHO. Influenza updates. Available at: https://www.who.int/influenza/surveillance_monitoring/updates/en/ Accessed 26 April 2020.

5. Zhou P, Yang XL, Wang XG, et al. A pneumonia outbreak associated with a new coronavirus of probable bat origin. Nature **2020**; 579(7798): 270-3.

6. CT C-J, M L, MJ K, MK R, V S. ACE2 and Microbiota: Emerging Targets for Cardiopulmonary Disease Therapy. Journal of cardiovascular pharmacology **2015**; 66(6): 540-50.

7. Jin X, Lian JS, Hu JH, et al. Epidemiological, clinical and virological characteristics of 74 cases of coronavirus-infected disease 2019 (COVID-19) with gastrointestinal symptoms. **2020**.

8. Du M, Cai G, Chen F, Christiani DC, Zhang Z, Wang M. Multi-omics Evaluation of Gastrointestinal and Other Clinical Characteristics of SARS-CoV-2 and COVID-19. Gastroenterology **2020**.

9. Gu J, Han B, Wang J. COVID-19: Gastrointestinal Manifestations and Potential Fecal-Oral Transmission. Gastroenterology **2020**.

10. Huttenhower C, Gevers D, Knight R, Abubucker S, H.Badger J. Structure, function and diversity of the healthy human microbiome. Nature 486(7402): p.207-14.

11. O'Hara AM, Shanahan F. The gut flora as a forgotten organ. EMBO reports **2006**; 7(7): 688-93.

12. Belkaid Y, Harrison OJ. Homeostatic Immunity and the Microbiota. Immunity **2017**; 46(4): 562-76.

13. Marsland BJ, Trompette A, Gollwitzer ES. The Gut-Lung Axis in Respiratory Disease. Annals of the American Thoracic Society **2015**; 12 Suppl 2: S150-6.

14. Wang J, Li F, Wei H, Lian ZX, Sun R, Tian Z. Respiratory influenza virus infection induces intestinal immune injury via microbiota-mediated Th17 cell-dependent inflammation. The Journal of experimental medicine **2014**; 211(12): 2397-410.

15. Ichinohe T, Pang IK, Kumamoto Y, et al. Microbiota regulates immune defense against respiratory tract influenza A virus infection. Proc Natl Acad Sci U S A **2011**; 108(13): 5354-9.

16. Gu S, Chen Y, Zhang X, et al. Identification of key taxa that favor intestinal colonization of Clostridium difficile in an adult Chinese population. Microbes & Infection **2016**; 18(1): 30-8.

17. National Health Commission of the People's Republic of China, National Administration of Traditional Chinese Medicine. Guideline for diagnosis and treatment of COVID-19 (7th version). Available at: http://www.nhc.gov.cn/yzygj/s7653p/202003/46c9294a7dfe4cef80dc7f5912eb1989.shtml Accessed 24 April 2020.

18. Fitzner J, Qasmieh S, Mounts AW, et al. Revision of clinical case definitions: influenza-like illness and severe acute respiratory infection. Bulletin of the World Health Organization **2018**; 96(2): 122-8.

19. PI C, G Z, S S, et al. Towards standards for human fecal sample processing in metagenomic studies. Nature biotechnology **2017**; 35(11): 1069-76.

20. Liaw A, Wiener M. Classification and Regression by RandomForest. Forest **2001**; 23.

21. WHO 2019 nCoV situation report. Available at: https://www.who.int/emergencies/diseases/novel-coronavirus-2019/situation-reports Accessed 23 May 2020.

22. Kong WH, Li Y, Peng MW, Kong DG, Yang XB, Wang L. SARS-CoV-2 detection in patients with influenza-like illness. **2020**.

23. Tang X, Du R, Wang R, et al. Comparison of Hospitalized Patients With ARDS Caused by COVID-19 and H1N1. Chest **2020**.

24. Yildiz S, Mazel-Sanchez B, Kandasamy M, Manicassamy B, Schmolke M. Influenza A virus infection impacts systemic microbiota dynamics and causes quantitative enteric dysbiosis. **2018**; 6(1): 9.

25. Groves HT, Cuthbertson L, James P, Moffatt MF, Cox MJ, Tregoning JS. Respiratory Disease following Viral Lung Infection Alters the Murine Gut Microbiota. Front Immunol **2018**; 9: 182.

26. Ramanan P, Barreto JN, Osmon DR, Tosh PK. Rothia bacteremia: a 10-year experience at Mayo Clinic, Rochester, Minnesota. J Clin Microbiol **2014**; 52(9): 3184-9.

27. Lu HF, Li A, Zhang T, et al. Disordered oropharyngeal microbial communities in H7N9 patients with or without secondary bacterial lung infection. Emerging microbes & infections **2017**; 6(12): e112.

28. Lin K, Lin S, Lin AN, Lin T, Htun ZM, Reddy M. A Rare Thermophilic Bug in Complicated Diverticular Abscess. Case reports in gastroenterology **2017**; 11(3): 569-75.

29. Nahum A, Filice G, Malhotra A. A Complicated Thread: Abdominal Actinomycosis in a Young Woman with Crohn Disease. Case reports in gastroenterology **2017**; 11(2): 377-81.

30. Qin N, Zheng B, Yao J, Guo L, Li L. Influence of H7N9 virus infection and associated treatment on human gut microbiota. Scientific Reports **2015**; 5(2): 14771.

31. E D, GM B, X H, et al. Influenza Virus Affects Intestinal Microbiota and Secondary Salmonella Infection in the Gut through Type I Interferons. PLoS pathogens **2016**; 12(5): e1005572.

32. Zheng S, Fan J, Yu F, et al. Viral load dynamics and disease severity in patients infected with SARS-CoV-2 in Zhejiang province, China, January-March 2020: retrospective cohort study. **2020**; 369: m1443.

33. Qin N, Zheng B, Yao J, et al. Influence of H7N9 virus infection and associated treatment on human gut microbiota. Sci Rep **2015**; 5: 14771.

34. Sencio V, Barthelemy A, Tavares LP, et al. Gut Dysbiosis during Influenza Contributes to Pulmonary Pneumococcal Superinfection through Altered Short-Chain Fatty Acid Production. Cell reports **2020**; 30(9): 2934-47.e6.

35. Trompette A, Gollwitzer ES, Pattaroni C, et al. Dietary Fiber Confers Protection against Flu by Shaping Ly6c(-) Patrolling Monocyte Hematopoiesis and CD8(+) T Cell Metabolism. Immunity **2018**; 48(5): 992-1005.e8.

36.   Haase S, Haghikia A, Wilck N, Müller DN, Linker RA. Impacts of microbiome metabolites on immune regulation and autoimmunity. Immunology **2018**; 154(2): 230-8.

37.   Antunes KH, Fachi JL, de Paula R, da Silva EF, Pral LP. Microbiota-derived acetate protects against respiratory syncytial virus infection through a GPR43-type 1 interferon response. **2019**; 10(1): 3273.

Figure legends

Figure 1. Changes in fecal microbial diversity and community structures in COVID-19 patients (n=30), H1N1 patients (n=24), and healthy controls (HC) (n=30). There were significant differences in the alpha diversity of the gut microbiota among the three groups based on the Shannon index (A) and Chao index (B). Venn diagram showing the overlap of open taxonomic units of the fecal microbiota across the three groups (C). Beta diversity results were assessed by principal coordinate analysis (PCoA) of Bray-Curtis distances (D). Each point represents one sample. Each color indicates a study group (purple, healthy controls; orange, COVID-19 patients; blue-green, H1N1 patients). Ternary plot depicting the number of genera (relative abundance >3%) enriched in the COVID-19, H1N1, and HC groups (E). Each circle represents one genus, and the size of the circle reflects relative abundance. *P* < 0.05 for all data.

Figure 2. Taxonomic differences in the fecal microbiota between COVID-19 patients, H1N1 patients, and healthy controls. Comparison of the relative abundance at the phylum (A), class (B), family (C), and genus (D) levels across the three groups. Each box represents an interquartile range (first and third quartiles) of taxa abundance, and the black line corresponds to median abundance. Vertical lines represent the variability in the abundance of each taxon. Each circle corresponds to extreme values in each taxon. $*p_{adjust} = 0.05–0.01$; $**p_{adjust} = 0.01–0.001$ and $***p_{adjust} < 0.001$.
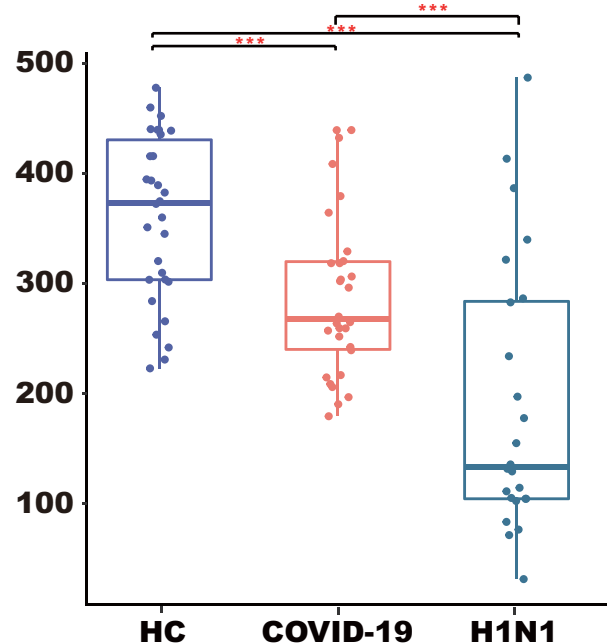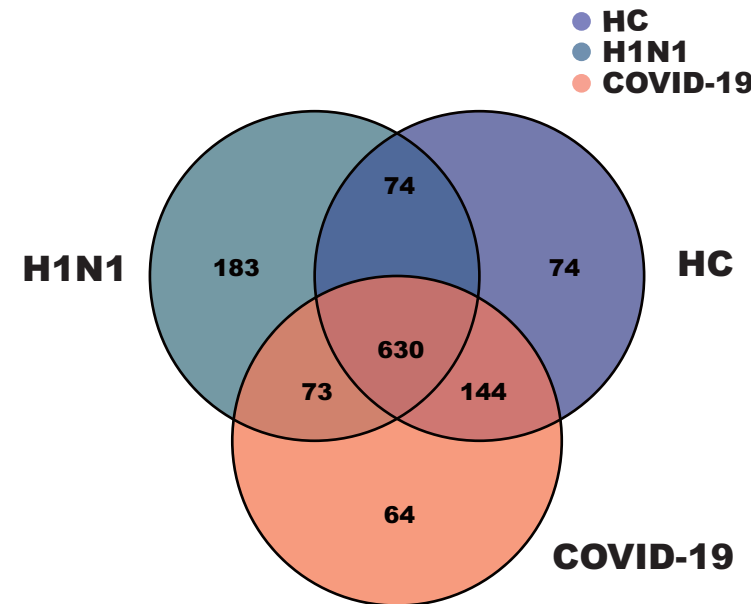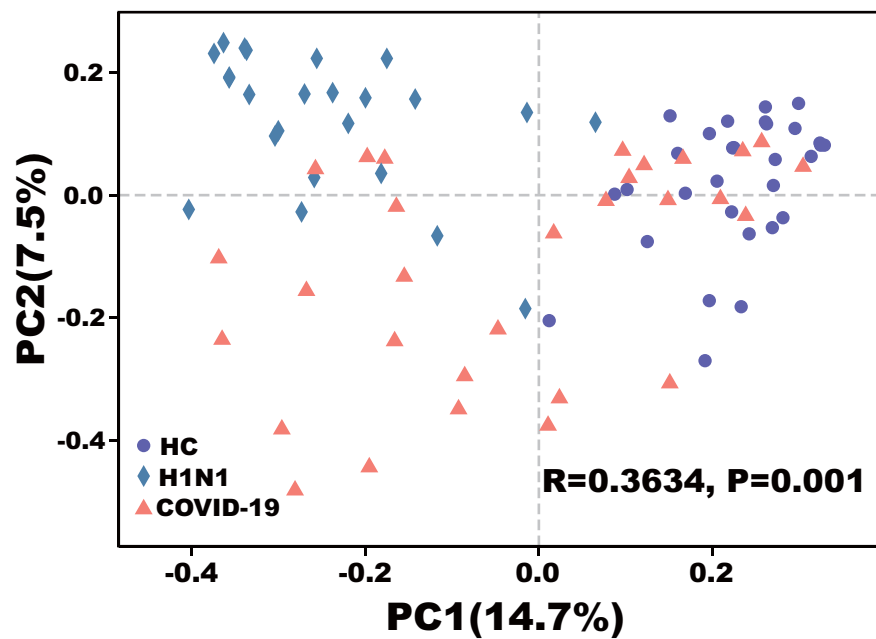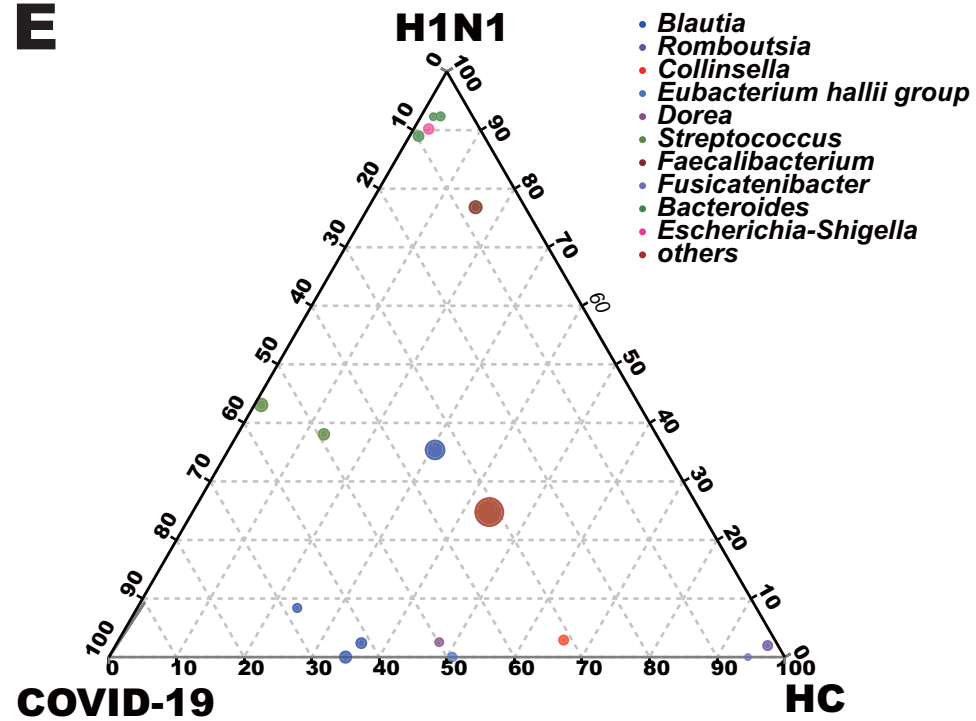
Figure 3. Linear discrimination analysis (LDA) effect size (LEfSe) analysis was used to identify differences in microbial composition between COVID-19 patients and healthy controls (HC) (A). At the genus level, LDA scores showed significant differences in microbiota composition between COVID-19 patients (blue) and HC (orange). Only taxa with an LDA threshold value >3.5 are shown. (B) Spearman correlation of associated genera in COVID-19 patients and HC. The genera enriched in COVID-19 patients (red text) were negatively correlated with HC-enriched genera (blue text). (C) Prediction of five biomarkers in the microbiome of COVID-19

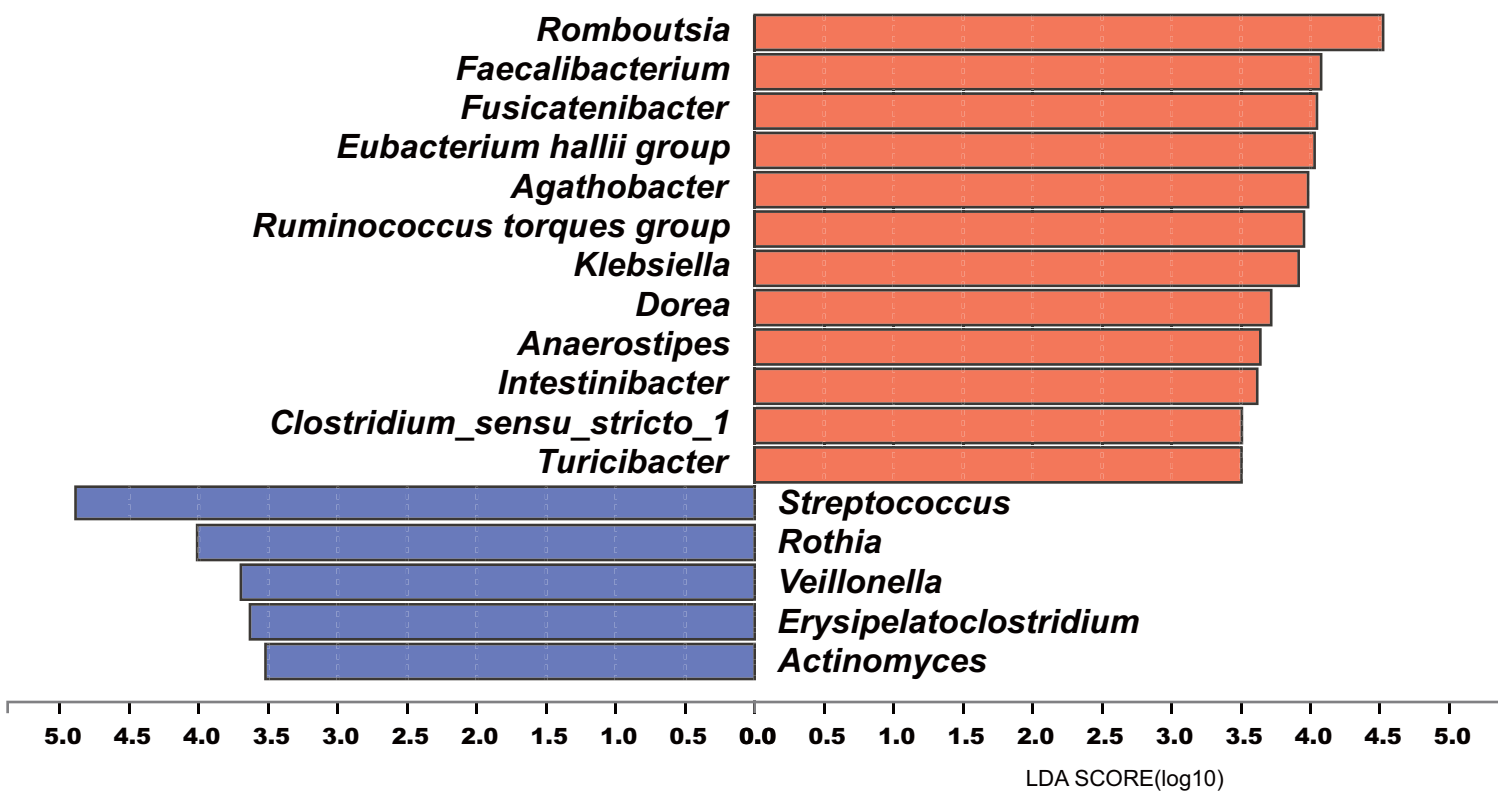patients and HC. The area under the receiver-operating characteristic (ROC) curve (AUC = 0.89) is shown in the center.

Figure 4. Linear discrimination analysis (LDA) effect size (LEfSe) analysis was used to differentiate the COVID-19 and H1N1 patients (A). At the genus level, LDA scores showed significant differences in microbiota composition between COVID-19 patients (orange) and H1N1 patients (blue). Only taxa with an LDA threshold >3.5 are shown. (B) Prediction of seven biomarkers in the microbiome of COVID-19 and H1N1 patients. The area under the receiver-operating characteristic (ROC) curve (AUC = 0.94) is shown in the center.
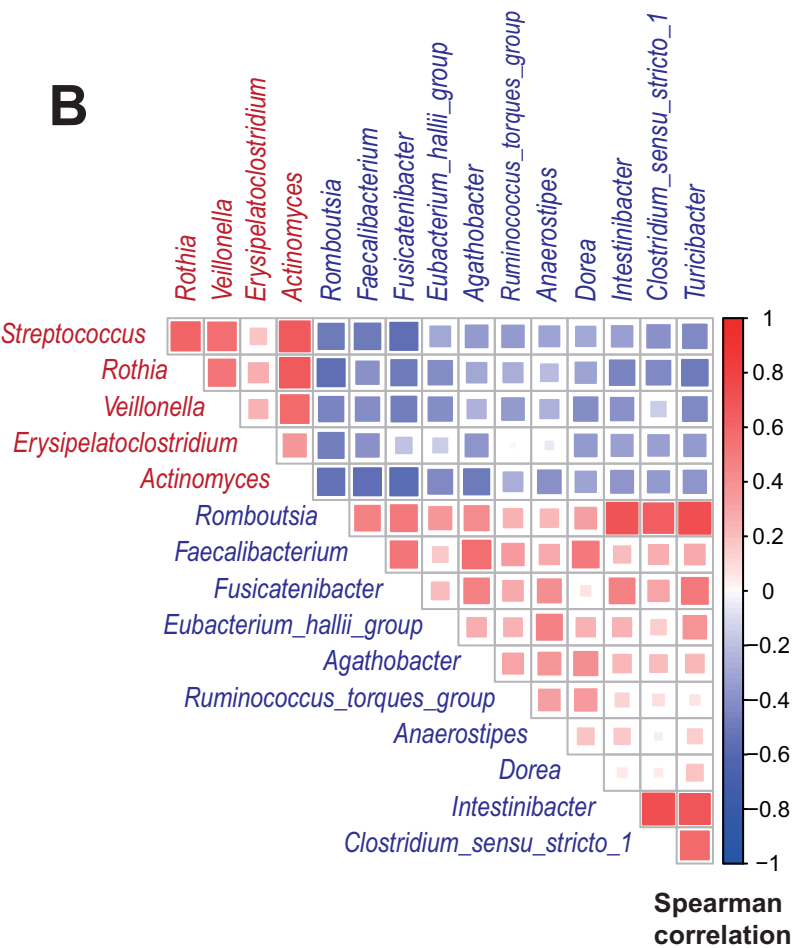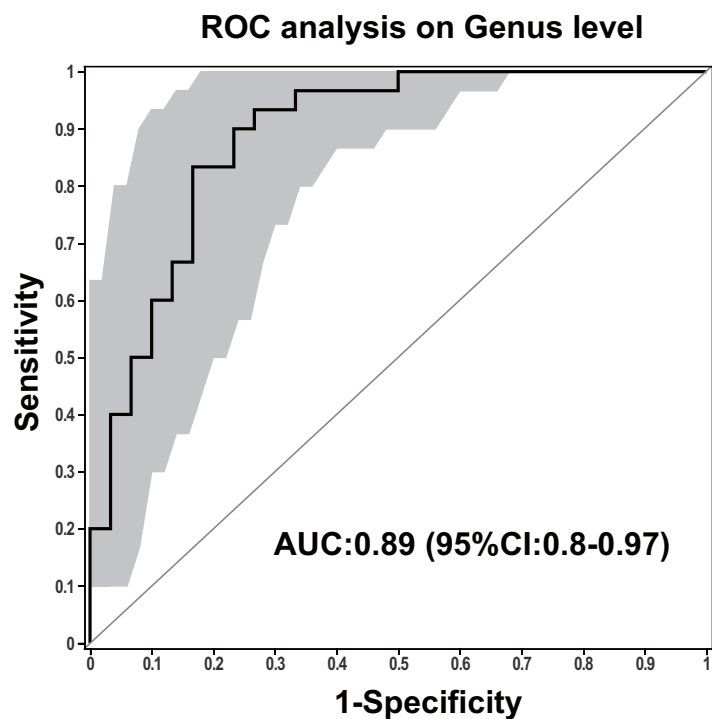
Figure 5. Association between genera composition and clinical indexes. Spearman analysis was conducted to evaluate the correlation between genera (abundance >0.1%) and inflammatory mediators and cytokines in COVID-19 (A) and H1N1 patients (B), respectively. Significance thresholds included absolute correlation coefficients higher than 0.4 and $P < 0.05$. Compared with the healthy controls (HC), the blue texts represent the significantly decreased genera and the red texts represent the significantly increased genera in patients. The degree of correlation is indicated by a color gradient from blue (negative correlation) to red (positive correlation).

A

COVID-19
H1N1

Prevotella
Ezakiella
Akkermansia
Murdochiella
Porphyromonas
Streptococcus
Blautia
Collinsella
Bifidobacterium
norank_f__Lachnospiraceae
Ruminococcus gnavus group
Anaerostipes
Dorea
Ruminococcus_2
Eubacterium hallii group
Agathobacter
Ruminococcus torques group
Rothia
Fusicatenibacter
Clostridium_sensu_stricto_1

5.0 4.5 4.0 3.5 3.0 2.5 2.0 1.5 1.0 0.5 0.0 0.5 1.0 1.5 2.0 2.5 3.0 3.5 4.0 4.5 5.0

LDA SCORE(log10)
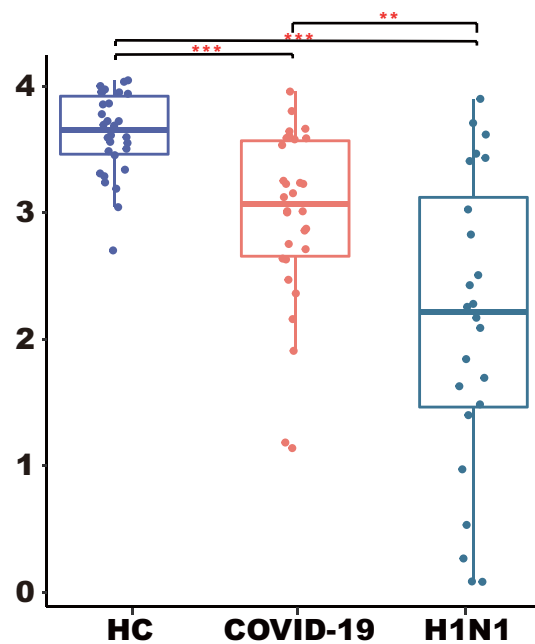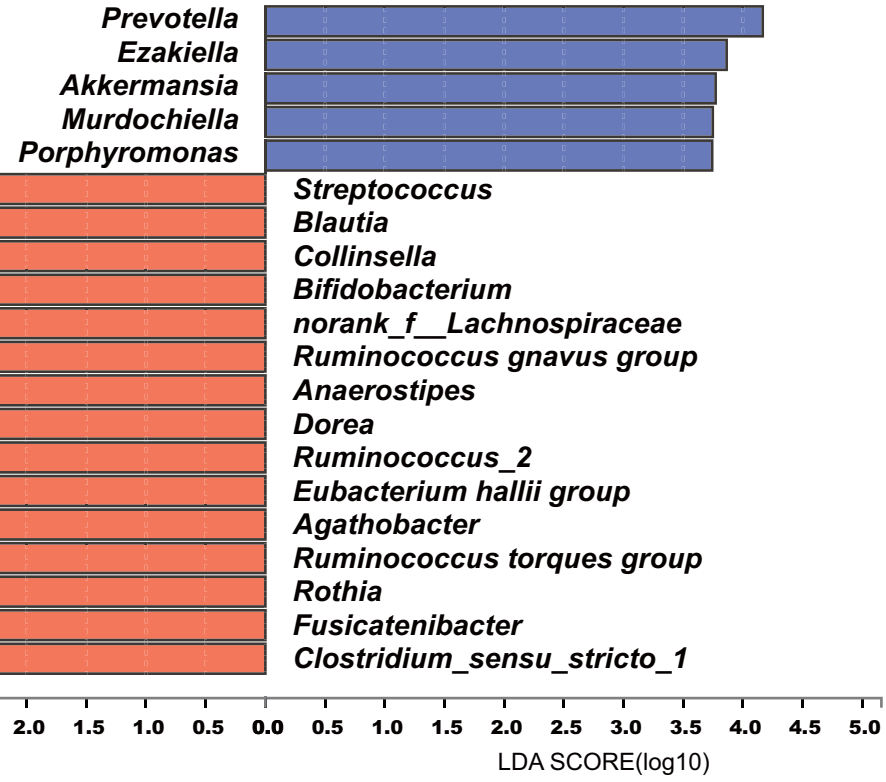
B

ROC analysis on Genus level
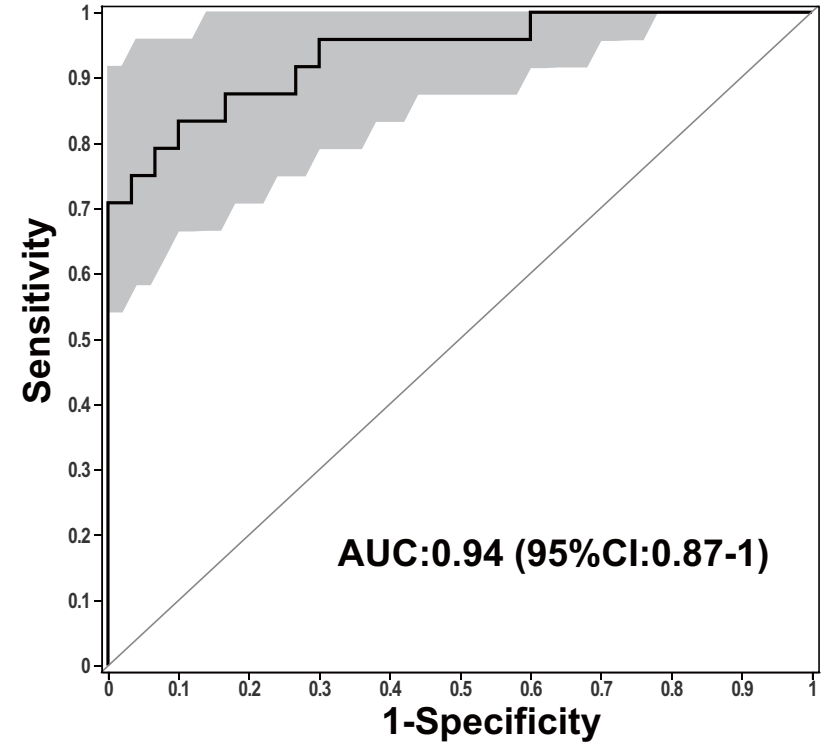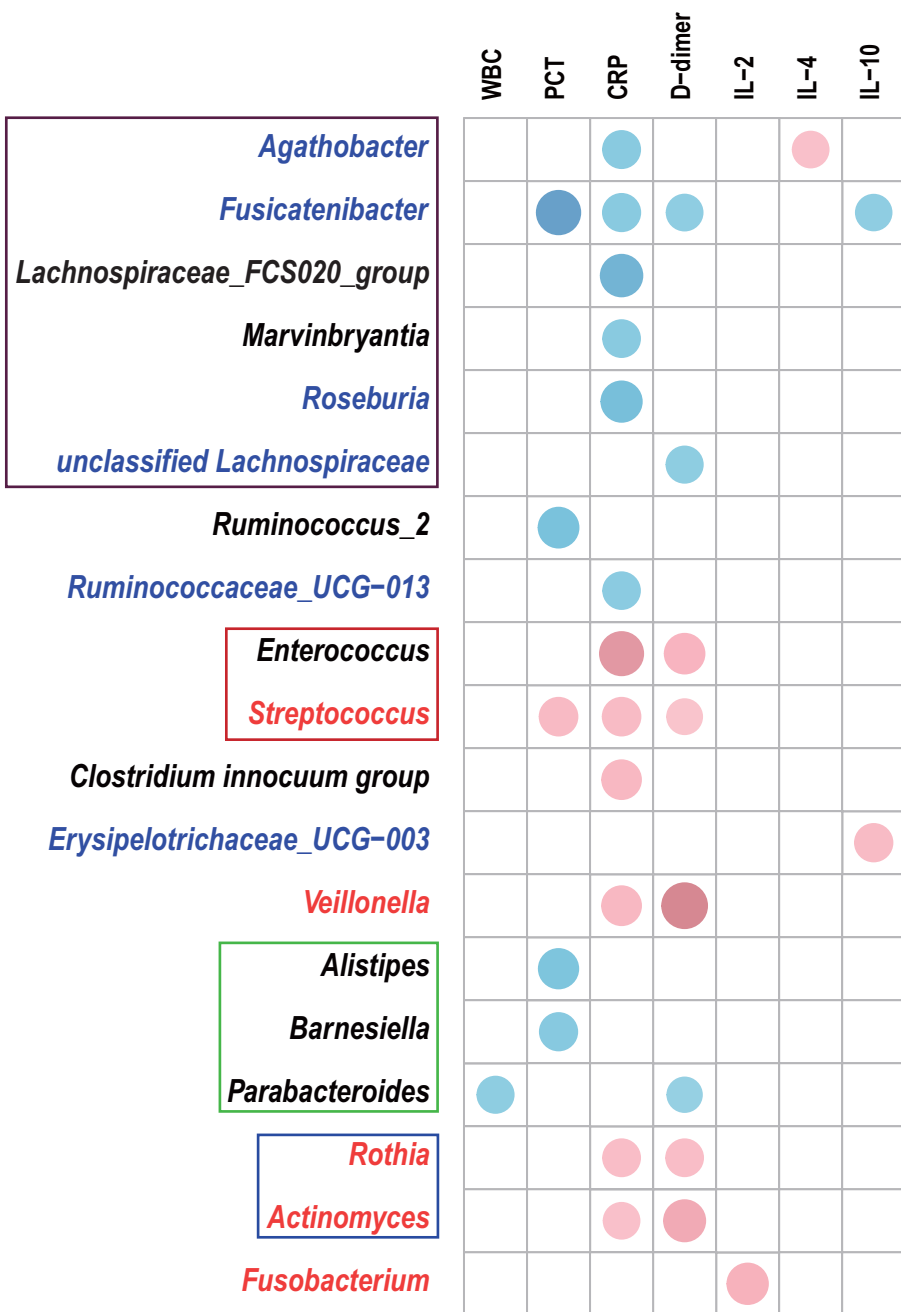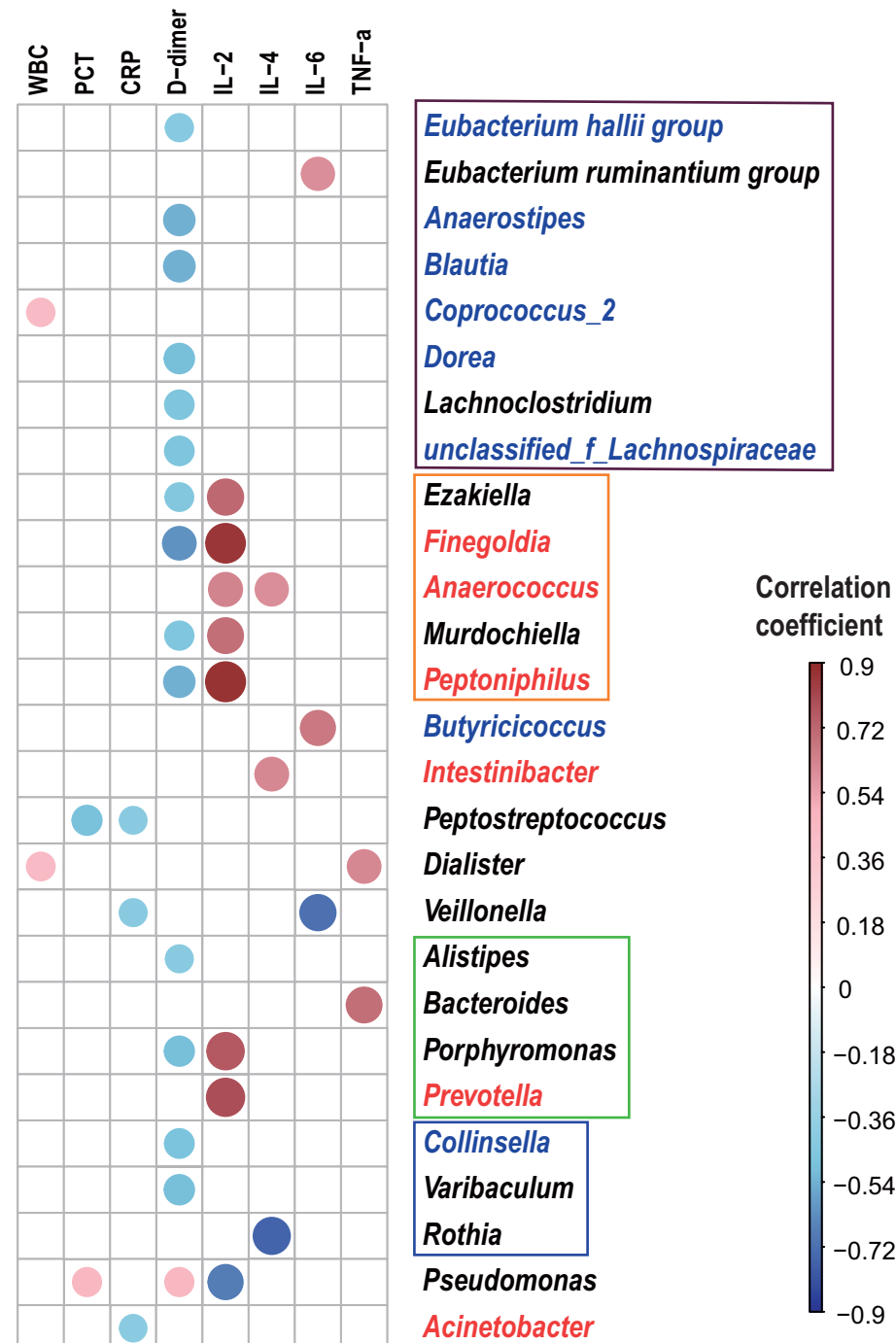
Sensitivity

1-Specificity

AUC:0.94 (95%CI:0.87-1)
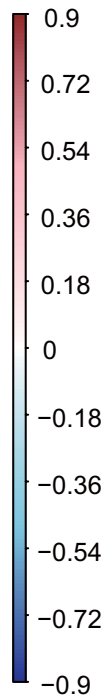
Table 1. Clinical characteristics of the study population.

	Healthy controls (N = 30)	H1N1 (N = 24)	COVID-19 (N = 30)	P-value[a]
Age, median (IQR), year	53.5 (43.8–60.3)	48.5 (33.3–66.8)	55.0 (48.0–62.0)	0.347
Female sex – no./total no. (%)	13/30 (43.3)	9/24 (37.5)	13/30 (43.3)	0.665
BMI, kg/m^2	22.9 (21.3–24.6)	24.5 (22.9–27.6)	24.6 (22.3–27.1)	0.993
Length of hospital stay	NA	7.0 (6.0–9.8)	16.0 (12.0–21.3)	<0.001
Coexisting disorder – no. (%)				
Any	NA	11/24 (45.8)	10/30 (33.3)	0.349
Hypertension	NA	5/24 (20.8)	9/30 (30.0)	0.445
Symptoms – no. (%)				
Fever on admission	NA	19/24 (79.2)	26/30 (86.7)	0.713
Temperature on admission (°C)	NA	38.2 (37.5–39.5)	38.2 (37.5–38.8)	0.632
Cough	NA	22/24 (91.7)	26/30 (86.7)	0.682
Diarrhea	NA	3/24 (12.5)	5/30 (16.7)	0.720
White blood cell count, ×10^9/L	5.9 (4.9–7.8)	6.1 (3.8–8.6)	6.2 (4.0–9.3)	0.801
Neutrophil count, ×10^9/L	3.4 (2.5–4.7)	4.7 (2.4–6.7)	4.6 (2.8–7.6)	0.459
Lymphocyte count, ×10^9/L	2.1 (1.4–2.5)	0.9 (0.6–1.4)[b]	0.9 (0.6–1.1)[b]	0.206
Platelet count, ×10^9/L	226.5 (204.3–249.5)	163.5 (128.8–230.5)[b]	206.0 (165.8–261.5)	0.026
Haemoglobin level, g/L	146.0 (140.0–152.3)	136.0 (123.5–152.5)	139.0 (124.8–151.0)[b]	0.882
C-reactive protein level ≥10 mg/L – no./total no. (%)	NA	18/24 (75.0)	21/29 (72.4)	0.832
Procalcitonin level ≥0.5 ng/ml – no./total no. (%)	NA	16/19 (84.2)	15/30 (50.0)	0.016
Alanine aminotransferase, U/L	15.0 (10.8–23.3)	28.0 (19.8–50.0)[b]	22.0 (15.8–38.5)[b]	0.188
Aspartate aminotransferase, U/L	19.0 (16.8–23.0)	36.0 (21.3–61.5)[b]	20.0 (16.0–39.5)	0.018

Lactate dehydrogenase, U/L	NA	258.0 (229.3–349.8)	243.5 (210.3–331.8)	0.331
Creatinine, μmol/L	69.5 (65.0–81.0)	62.5 (53.3–81.3)	77.0 (62.8–84.8)	0.083
D-dimer, mg/L	NA	533.0 (186.0–1546.0)	274.0 (174.0–442.5)	0.107
IL-2, pg/mL	0.9 (0.9–0.9)	1.5 (1.4–1.7)[b]	1.0 (0.9–1.7)[b]	0.065
IL-4, pg/mL	1.2 (1.2–1.2)	1.4 (1.2–1.7)[b]	1.8 (1.8–1.9)[b]	0.003
IL-6, pg/mL	2.0 (2.0–2.1)	11.0 (5.3–15.9)[b]	19.9 (9.2–42.1)[b]	0.097
IL-10, pg/mL	0.8 (0.7–0.8)	3.6 (2.5–4.2)[b]	4.3 (3.1–7.8)[b]	0.124
TNF-α, pg/mL	3.6 (3.6–3.9)	4.4 (4.1–4.4)[b]	22.3 (12.2–73.8)[b]	<0.001

Abbreviations: NA, not available; IQR, interquartile range; BMI, body mass index; IL, interleukin; TNF-α, tumor necrosis factor-α.

[a] P values indicate differences between H1N1 and COVID-19. $P < 0.05$ was considered statistically significant.

[b] $P < 0.05$ was considered to indicate significant difference between healthy controls and H1N1 and COVID-19, respectively.